JOC*Article*

Conformational Analysis of Nine-Membered Cyclic Acetals. Stereoelectronic Effect in 2,4- and 3,5-Benzodioxonine Derivatives

Wojciech Migda and Barbara Rys*

Department of Organic Chemistry, Jagiellonian University, Ingardena 3, 30-060 Kraków, Poland

rys@chemia.uj.edu.pl

Received February 28, 2006

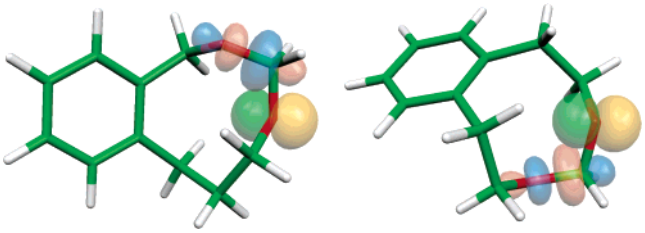

Conformations of the title compounds were examined using DFT calculations and NBO analysis in order to find the origins of their conformational preferences. The most stable conformations were TBC and TCBtype-1 for the 2,4- and 3,5-benzodioxonine derivatives, respectively. In both of these conformations the acetal moiety adopts the $g\pm g\pm$ geometry. The NBO analysis yielded values of the stabilization energy associated with the stereoelectronic $n_O \rightarrow \sigma_{C-O}^*$ interactions that were highest for conformations other than the global minima. Conformers displaying the strongest interactions followed different patterns of atom arrangement within the acetal moiety, namely $g+g-$, and those in which one or both of the torsion angles within the C−O−C−O−C segment were close to 90°. Steric repulsion caused by alkyl substituents at the anomeric carbon was found to influence the strength of the $n_O \rightarrow \sigma_{C-O}^*$ stabilization through modification of bond lengths and torsion angles. The adopted ground-state conformations result from accommodation of steric repulsions and stabilizing stereoelectronic interactions. It was shown that DFT calculations of conformational preferences of acetals together with GIAO prediction of ^{13}C chemical shifts should be a useful methodology for studies on conformation and conformational equilibria of acetals in solution.

Introduction

For the last five decades the stereoelectronic effect, being one of the key structural factors recognized in a vast number of natural and synthetic compounds, has attracted considerable attention among both experimental and theoretical chemists.[1,2] Numerous attempts have been undertaken to investigate consequences and to understand the origin and nature of this effect. Experimental methods are by far more common in studying modifications to the geometrical and thermodynamical parameters affected by the stereoelectronic effect,[3−8] while the theoretical approach is the method of choice to investigate the fundamental mechanisms underlying this phenomenon.[9−14]

Conformational preferences of the acetal moiety C−O−C−

(1) Juaristi, E.; Cuevas, G. *Tetrahedron* **1992**, *48*, 5019−5087.
(2) Graczyk, P. P.; Mikołajczyk, M. *Top. Stereochem.* **1994**, *21*, 159−349.
(3) Anderson, J. E. *J. Org. Chem.* **2000**, *65*, 748−754.
(4) Venkatesan, V.; Sundararajan, K.; Sankaran, K.; Viswanathan, K. S. *Spectrochim. Acta, Part A* **2002**, *58*, 467−478.
(5) Venkatesan, V.; Sundararajan, K.; Viswanathan, K. S. *J. Phys. Chem. A* **2002**, *106*, 7707−7713.
(6) Venkatesan, V.; Sundararajan, K.; Viswanathan, K. S. *Spectrochim. Acta, Part A* **2003**, *59*, 1497−1507.
(7) Favero, L. B.; Caminati, W.; Velino, B. *Phys. Chem. Chem. Phys.* **2003**, *5*, 4776−4779.
(8) Chen, Y.-Y.; Luo, S.-Y.; Hung, S.-C.; Chan, S. I.; Tzou, D.-L. M. *Carbohydr. Res.* **2005**, *340*, 723−729.
(9) (a) Salzner, U.; Schleyer, P. v. R. *J. Org. Chem.* **1994**, *59*, 2138−2155. (b) Salzner, U. *J. Org. Chem.* **1995**, *60*, 986−995. (c) Carballeira, L.; Pérez-Juste, I. *J. Org. Chem.* **1997**, *62*, 6144−6151.
(10) Alabugin, I. V. *J. Org. Chem.* **2000**, *65*, 3910−3919.
(11) Cortés, F.; Tenorio, J.; Collera, O.; Cuevas, G. *J. Org. Chem.* **2001**, *66*, 2918−2924.
(12) Alabugin, I. V.; Manoharan, M.; Zeidan, T. A. *J. Am. Chem. Soc.* **2003**, *125*, 14014−14031.
(13) Hetényi, A.; Martinek, T. A.; Lázár, L.; Zalán, Z.; Fülöp, F. *J. Org. Chem.* **2003**, *68*, 5705−5712.
(14) Martinez, K.; Cortes, F.; Leal, I.; Reyna, V.; Quintana, D.; Antúnez, S.; Cuevas, G. *Arkivoc* **2003**, *11*, 132−148.

10.1021/jo060422c CCC: $33.50
Published on Web 06/27/2006

O−C are in principle governed by a stereoelectronic effect defined as a delocalization of an oxygen lone pair into a C−O antibonding orbital ($n_O \rightarrow \sigma_{C-O}^*$). The highest stability of such a fragment is a consequence of the most effective overlap between the above-mentioned orbitals, which can be achieved for either a gauche+/gauche+ (*g*+*g*+) or gauche+/*gauche*− (*g*+*g*−) atom arrangement. However, the *g*+*g*− orientation is usually strongly destabilized by unfavorable steric repulsion, as in the case of dimethoxymethane.[4] A third conformation of the acetal fragment, with characteristic alignment of the C−H bond and the vicinal O−R part in the O−CHR′−OR fragment, named *anomeric eclipsed*, was recognized by Anderson.[3] This conformation is a result of a compromise between steric and stereoelectronic interactions in acetals bearing single bulky substituents at the anomeric carbon.

Incorporation of the acetal moiety into the ring system may restrict its ability to adopt the *g*+*g*+ geometry. However, with the increasing size of the ring, its flexibility becomes much higher, and in eight-membered and larger rings the two adjacent torsion angles may attain the *g*+*g*+ arrangement.

The question of conformational preferences and equilibria in conformationally flexible systems with low barriers for conformational processes in most cases can be answered by application of variable-temperature NMR measurements.[15−20] The alternative approach involves the prediction of NMR spectra of a set of computationally generated conformers and subsequent comparison with experimental data.[18e,21,22] The aim of our research was to perform conformational analysis of nine-membered cyclic acetals by combined use of experimental and computational methods and to determine whether the stereoelectronic effect is one of the key factors that decide the conformational preferences of these systems.

Computational Methods

Conformational space for all compounds was explored using the molecular mechanics method and the MMP3(2000) force field as implemented in the Tinker program.[23] In subsequent geometry optimizations, the B3LYP density functional was employed. For carbon and hydrogen atoms the 6-31G(d,p) basis set was used, which was augmented with extra diffusion functions for oxygen atoms, 6-31+G(d). Energy minima were confirmed by vibrational analysis, which in all cases showed no imaginary frequencies. Enthalpy and free-energy values were calculated for the standard conditions and were not scaled. Relative populations of conformers were estimated on the basis of the Boltzmann distribution at 298 K. ^{13}C NMR shielding constants were calculated with the mPW1PW91 density functional and the 6-311G(d,p) basis set using the GIAO method. Values of the shieldings were scaled into chemical shifts using an empirical formula.[24] NBO analysis was carried out at the Hartree−Fock level using the same basis set as in the geometry optimizations. The energy of the $n_O \rightarrow \sigma_{C-O}^*$ delocalization was derived by means of selective deletion of off-diagonal blocks of the Fock matrix.

MM computations were carried out with the SCAN and NEWTON programs from the Tinker 4.1 package.[25] All gas-phase DFT calculations were done with the Gaussian 03 program.[26] NBO computations were performed using the NBO 5.0 program[27] within the NWChem 4.6 suite.[28] Cartesian and spherical basis functions were used in geometry/NBO and ^{13}C magnetic shielding calculations, respectively.

Results and Discussion

Cyclization Reactions. The nine-membered acetals **1a**−**d** and **2a**−**d** were prepared in the acid-catalyzed condensation of the respective diol **3** or **4** and the carbonyl compound. Since formation of the nine-membered rings is particularly disfavored due to disadvantageous enthalpic and entropic factors,[29] the

(15) (a) Anet, F. A. L.; Degen, P. J. *J. Am. Chem. Soc.* **1972**, *94*, 1390−1392. (b) Anet, F. A. L.; Degen, P. J.; Krane, J. *J. Am. Chem. Soc.* **1976**, *98*, 2059−2066. (c) St-Amour, R.; Phan Viet, M. T.; St-Jacques, M. *Can. J. Chem.* **1984**, *62*, 2830−2840. (d) St-Amour, R.; St-Jacques, M. *Tetrahedron Lett.* **1985**, *26*, 13−16.

(16) Selzer, T.; Rappoport, Z. *J. Org. Chem.* **1996**, *61*, 7326−7334.

(17) Brown, J. H.; Bushweller, H. *J. Phys. Chem. A* **1997**, *101*, 5700−5706.

(18) (a) Pawar, D. M.; Noe, E. A. *J. Am. Chem. Soc.* **1998**, *120*, 1485−1488. (b) Pawar, D. M.; Noe, E. A. *J. Am. Chem. Soc.* **1998**, *120*, 5312−5314. (c) Pawar, D. M.; Miggins, S. D.; Smith, S. V.; Noe, E. A. *J. Org. Chem.* **1999**, *64*, 2418−2421. (d) Pawar, D. M.; Davis, K. L.; Brown, B. L.; Smith, S. V.; Noe, E. A. *J. Org. Chem.* **1999**, *64*, 4580−4585. (e) Pawar, D. M.; Moody, E. M.; Noe, E. A. *J. Org. Chem.* **1999**, *64*, 4586−4589.

(19) Bangerter, F.; Karpf, M.; Meier, L. A.; Rys, P.; Skrabal, P. *J. Am. Chem. Soc.* **1998**, *120*, 10653−10659.

(20) (a) Braverman, S.; Zafrani, Y.; Gottlieb, H. E. *J. Org. Chem.* **2002**, *67*, 3277−3283. (b) Belostotskii, A. M.; Gottlieb, H. E.; Shokhen, M. *J. Org. Chem.* **2002**, *67*, 9257−9266.

(21) (a) Stahl, M.; Schopfer, U. *J. Chem. Soc., Perkin Trans. 2* **1997**, 905−908. (b) Weston, J.; Ahlbrecht, H. *J. Chem. Soc., Perkin Trans. 2* **1997**, 1003−1006.

(22) (a) Forsyth, D. A.; Sebag, A. B. *J. Am. Chem. Soc.* **1997**, *119*, 9483−9494. (b) Sebag, A. B.; Friel, C. J.; Hanson, R. N.; Forsyth, D. A. *J. Org. Chem.* **2000**, *65*, 7902−7912. (c) Sebag, A. B.; Forsyth, D. A.; Plante, M. A. *J. Org. Chem.* **2001**, *66*, 7967−7973.

(23) (a) Allinger, N. L.; Yuh, Y. H.; Lii, J. H. *J. Am. Chem. Soc.* **1989**, *111*, 8551−8566. (b) Allinger, N. L.; Yuh, Y. H.; Lii, J. H. *J. Am. Chem. Soc.* **1989**, *111*, 8566−8575. (c) Allinger, N. L.; Yuh, Y. H.; Lii, J. H. *J. Am. Chem. Soc.* **1989**, *111*, 8575−8582.

(24) Migda, W.; Rys, B. *Magn. Reson. Chem.* **2004**, *42*, 459−466.

(25) Pappu, R. V.; Hart, R. K.; Ponder, J. W. *J. Phys. Chem. B* **1998**, *102*, 9725−9742.

(26) Frisch, M. J.; Trucks, G. W.; Schlegel, H. B.; Scuseria, G. E.; Robb, M. A.; Cheeseman, J. R.; Montgomery, J. A., Jr.; Vreven, T.; Kudin, K. N.; Burant, J. C.; Millam, J. M.; Iyengar, S. S.; Tomasi, J.; Barone, V.; Mennucci, B.; Cossi, M.; Scalmani, G.; Rega, N.; Petersson, G. A.; Nakatsuji, H.; Hada, M.; Ehara, M.; Toyota, K.; Fukuda, R.; Hasegawa, J.; Ishida, M.; Nakajima, T.; Honda, Y.; Kitao, O.; Nakai, H.; Klene, M.; Li, X.; Knox, J. E.; Hratchian, H. P.; Cross, J. B.; Bakken, V.; Adamo, C.; Jaramillo, J.; Gomperts, R.; Stratmann, R. E.; Yazyev, O.; Austin, A. J.; Cammi, R.; Pomelli, C.; Ochterski, J. W.; Ayala, P. Y.; Morokuma, K.; Voth, G. A.; Salvador, P.; Dannenberg, J. J.; Zakrzewski, V. G.; Dapprich, S.; Daniels, A. D.; Strain, M. C.; Farkas, O.; Malick, D. K.; Rabuck, A. D.; Raghavachari, K.; Foresman, J. B.; Ortiz, J. V.; Cui, Q.; Baboul, A. G.; Clifford, S.; Cioslowski, J.; Stefanov, B. B.; Liu, G.; Liashenko, A.; Piskorz, P.; Komaromi, I.; Martin, R. L.; Fox, D. J.; Keith, T.; Al-Laham, M. A.; Peng, C. Y.; Nanayakkara, A.; Challacombe, M.; Gill, P. M. W.; Johnson, B.; Chen, W.; Wong, M. W.; Gonzalez, C.; Pople, J. A. *Gaussian 03*, revision C.02; Gaussian, Inc.: Wallingford, CT, 2004.

(27) (a) Foster, J. P.; Weinhold, F. *J. Am. Chem. Soc.* **1980**, *102*, 7211−7218. (b) Glendening, E. D.; Badenhoop, J. K.; Reed, A. E.; Carpenter, J. E.; Bohmann, J. A.; Morales, C. M.; Weinhold, F. *NBO 5.0*; Theoretical Chemistry Institute, University of Wisconsin: Madison, WI, 2001.

(28) Straatsma, T. P.; Aprà, E.; Windus, T. L.; Bylaska, E. J.; de Jong, W.; Hirata, S.; Valiev, M.; Hackler, M. T.; Pollack, L.; Harrison, R. J.; Dupuis, M.; Smith, D. M. A.; Nieplocha, J.; Tipparaju, V.; Krishnan, M.; Auer, A. A.; Brown, E.; Cisneros, G.; Fann, G. I.; Fruchtl, H.; Garza, J.; Hirao, K.; Kendall, R.; Nichols, J. A.; Tsemekhman, K.; Wolinski, K.; Anchell, J.; Bernholdt, D.; Borowski, P.; Clark, T.; Clerc, D.; Dachsel, H.; Deegan, M.; Dyall, K.; Elwood, D.; Glendening, E.; Gutowski, M.; Hess, A.; Jaffe, J.; Johnson, B.; Ju, J.; Kobayashi, R.; Kutteh, R.; Lin, Z.; Littlefield, R.; Long, X.; Meng, B.; Nakajima, T.; Niu. S.; Rosing, M.; Sandrome, G.; Stave, M.; Taylor, H.; Thomas, G.; van Lenthe, J.; Wong, A.; Zhang, Z. *NWChem, A Computational Chemistry Package for Parallel Computers*, version 4.6; Pacific Northwest National Laboratory: Richland, WA, 2004.

(29) Eliel, E. L.; Wilen, S. H. *Stereochemistry of Organic Compounds*; Wiley: New York, 1994.

medium dilution conditions were applied in the synthetic procedure (for details, see Supporting Information). For the 26−37 mM diol concentrations, the products were isolated in 7−65% yields. The acetal **2a** was previously synthesized in our laboratory.[30]

^{13}C NMR Signal Assignments. Spectral assignment of ^{13}C NMR signals, which was crucial for the successful completion of the conformational analysis, was accomplished on the basis of 1D and 2D NMR spectra analysis. Further details are available in Supporting Information.

Computational Studies. To study the influence of the stereoelectronic effect on the conformational preferences of acetals **1a**−**d** and **2a**−**d**, a comprehensive theoretical investigation was carried out. The first step involved molecular mechanics exploration of the conformational space, which for each compound provided initial geometries of the local minima. These conformations were then subjected to a further full geometry optimization in the gas phase using DFT methods. Vibrational analysis applied to the stationary points found in that manner proved that all of them are true minima and provided values of standard enthalpy and free energy (H_{298}^0 and G_{298}^0).

In the second step, we wanted to learn whether the conformational picture obtained from gas-phase DFT geometry computations agrees with the situation observed in solution. For this purpose, the ^{13}C NMR spectra were calculated for the conformers within the range of 10 kJ/mol and compared either individually or as a Boltzmann-weighted average, with the experimental chemical shifts. Statistical evaluation of the agreement was applied to draw relevant conclusions.

After completion of the conformational analysis, NBO calculations at the Hartree−Fock level were carried out. In this step, the magnitude of the $n_O \rightarrow \sigma_{C-O}^*$ orbital interactions, which are responsible for the stereoelectronic effect in acetals, was evaluated.

A. Geometry Modeling. The conformational analysis of *Z*-cyclononene carried out using theoretical methods revealed 13 different types of conformers in the energy window of 30 kJ/mol.[31] We have obtained similar results for benzocyclononene, the parent carbocyclic system of our acetals. The geometry of the global minimum of both compounds is the same, TCBtype-1, but the benzannelation modifies the energy order and free-energy differences between conformers. We have not located, however, the TCBtype-4 conformer described by Glaser, but instead we have found another energy minimum of benzocyclononene. Following the original naming scheme[31] this conformer, due to its resemblance of the twist−chair−chair conformer of cyclononane, should be assigned the TCC descriptor, which unfortunately is already in use by another energy minimum. To avoid ambiguity, the new conformer was named TCCtype-2 and the other, from Glaser's work, TCCtype-1.

Calculations performed for the molecules of the title compounds showed that although conformational space of their molecules is similarly complicated, the global minima are more separated from the following conformers (Table 1).

The ground-state conformation adopted by molecules of compounds **1a**−**d** is in a series virtually the same and can be described as twist−boat−chair (TBC) following the nomenclature proposed by Glaser et al. for nine-membered rings.[31]

TABLE 1. Relative Free Energies, Enthalpies, Electronic Energies (kJ/mol), and Populations of Conformers of Compounds 1a−d and 2a−d Calculated Using the B3LYP/6-31G (O, 6-31+G*) Method**

	conformer	ΔG_{298}^0	ΔH_{298}^0	ΔE	population %
1a	1,TBC(−)	0.00	0.00	0.00	83.2
	2,TCBtype-2(+)	5.54	6.70	7.23	8.9
	3,SCBtype-3	6.72	6.45	6.25	5.5
1b	1,TBC(−)	0.00	0.00	0.00	53.8
	2,TBC(−)	0.94	0.88	0.86	36.8
	3,TCBtype-3(+)	7.13	8.70	9.45	3.0
	4,SCBtype-3	8.35	8.23	8.40	1.8
	5,TCBtype-2(+)	8.80	9.70	10.38	1.5
1c	1,TBC(−)	0.00	0.00	0.00	99.2
1d	1,TBC(−)	0.00	0.00	0.00	29.7
	2,TCBtype-3(+)	0.14	1.38	2.30	28.0
	3,TBC(−)	1.01	1.42	1.76	19.8
	4,SCBtype-1	2.92	4.11	4.26	9.1
	5,TCCtype-1(−)	3.60	5.64	6.84	6.9
	6,TCBtype-1(+)	4.94	5.66	6.20	4.0
	7,TCBtype-2(+)	7.96	9.27	10.16	1.2
	8,SCBtype-3	9.81	9.82	9.94	0.6
2a	1,TCBtype-1	0.00	0.00	0.00	99.9
2b	1,TCBtype-1	0.00	0.00	0.00	71.5
	2,TCBtype-1	2.37	2.41	2.31	27.5
2c	1,TCBtype-1	0.00	0.00	0.00	99.5
2d	1,TCBtype-1	0.00	0.00	0.00	51.6
	2,SCC	2.27	4.41	5.47	20.7
	3,TCCtype-1	2.28	4.88	5.97	20.6
	4,TCBtype-1	6.61	7.23	6.96	3.6
	5,TCBtype-3	9.46	11.59	12.51	1.1
	6,TCBtype-2	9.70	9.59	9.50	1.0

SCHEME 1. Nine-Membered Acetals Studied in This Work

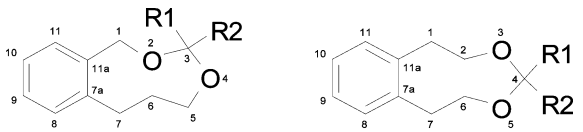

1 **2**

	a	b	c	d
R1:	H	Me	Me	*t*-Bu
R2:	H	H	Me	H

However, replacement of either the C-2 or C-6 carbon atoms by oxygen in the TBC conformer of the parent carbocycle leads to two different conformations (for numbering, see Scheme 1). The same is true for all C_1 symmetrical conformations of the nine-membered ring. To distinguish them we have systematically added a suffix, either (+) or (−), to the descriptor of the conformation (the former corresponds to the substitution of C-2).

For the unsubstituted system and its methyl derivatives (**1a**−**c**), the TBC(−) conformation dominates the population of molecules. In **1a** it constitutes over 83% of the population, in **1b**, represented by the two conformers with an opposite orientation of the substituent, it comprises 91%, while in **1c** the structures with higher energy provide less than 1%. This picture is, however, in marked contrast with the situation displayed for **1d**, the derivative bearing the large *tert*-butyl substituent. Here also the TBC(−) conformation is the global minimum, but it is populated to the extent of less than one-third. Together with the third lowest free-energy conformer, which differs only in the substituent orientation, they constitute half of the population.

Molecules of the second group of compounds (**2a**−**d**) prefer the TCBtype-1 (twist−chair−boat) conformation, the global

(30) Rys, B.; Szneler, E.; Duddeck, H. *Liebigs Ann.* **1996**, 701−704.
(31) Glaser, R.; Shiftan, D.; Levi-Roso, G.; Ergaz, I.; Geresh, S.; Drouin, M. *J. Org. Chem.* **2002**, *67*, 5486−5496.

TABLE 2. Experimental and Calculated Chemical Shifts, Their Differences, and Parameters of Statistical Evaluation of δ_{expt} vs δ_{calcd}[a]

		1		2		3		1 + 2 + 3	
nucleus	δ_{expt}	δ_{calcd}	$\lvert\Delta\delta\rvert$	δ_{calcd}	$\lvert\Delta\delta\rvert$	δ_{calcd}	$\lvert\Delta\delta\rvert$	δ_{calcd}	$\lvert\Delta\delta\rvert$
C1	66.8	66.3	0.5	74.3	7.5	67.3	0.5	67.1	0.3
C3	93.3	92.4	0.9	94.1	0.8	95.3	2.0	92.7	0.6
C5	61.5	58.9	2.6	68.5	7.0	70.5	9.0	60.4	1.1
C6	30.1	31.6	1.5	34.1	4.0	33.3	3.2	31.9	1.8
C7	28.2	29.9	1.7	33.2	5.0	28.9	0.7	30.2	2.0
C7a	140.7	141.1	0.4	146.2	5.5	145.6	4.9	141.8	1.1
C8	130.6	130.8	0.2	130.2	0.4	129.8	0.8	130.7	0.1
C9	128.8	128.9	0.1	128.6	0.2	128.6	0.2	128.9	0.1
C10	126.5	126.7	0.2	125.3	1.2	126.2	0.3	126.5	0.0
C11	130.8	132.4	1.6	128.2	2.6	131.0	0.2	131.9	1.1
C11a	137.2	138.6	1.4	137.8	0.6	137.0	0.2	138.4	1.2
$\lvert\Delta\delta\rvert_{max}$			2.6		7.5		9.0		2.0
$\lvert\Delta\delta\rvert_{avg}$			1.0		3.2		2.0		0.9
regr. err.			1.4		3.0		3.0		1.0
r^2			0.999		0.996		0.996		1.000

[a] Agreement obtained for the three most populated conformers of **1a** and their Boltzmann-weighted mixture. All data except r^2 in ppm.

minimum of the parent carbocycle. Similar to that in the case of **1a**−**d**, the conformational behavior of the *tert*-butyl derivative (**2d**) differs from the others (**2a**−**c**). While the population of the TCBtype-1 conformation in **2a**−**c** exceeds 98−99%, its fraction in **2d** is only 56%.

Conformations of the global minima of compounds **1a**−**d** and **2a**−**d** exhibit one common structural feature. The acetal moieties adopt the *gauche*±/*gauche*± (*g*±*g*±) arrangements, characteristic for the generalized anomeric effect (Supporting Information Tables S11−S18). This is also true for the two other less populated conformers of **1a**. Several conformers of the two *tert*-butyl derivatives (**1d** and **2d**) have a different arrangement in the acetal fragment. One of the two C−O−C−O torsion angles values is close to the gauche orientation, whereas the other has an opposite sign and is equal to ca. 120° (Supporting Information Tables S14 and S18). Such a geometry resembles the *anomeric eclipsed* conformation, in which steric interactions between the bulky *tert*-butyl substituent and the vicinal CH_2 groups are minimized.[3]

Stereoelectronic effects in the molecule modify not only its torsion angles, but also the bond lengths. The gauche orientation in the C−O−C−X fragment causes shortening of the bond between the oxygen and anomeric carbon and lengthening of the C−X bond. For the gauche/gauche orientation in acetals, this effect leads to averaging of the bond lengths in the O−C−O fragment.

In ground-state conformations of compounds **1a** and **2a**, the bond between the anomeric carbon and its neighboring oxygens is shortened to 1.408 and 1.405 Å, respectively, which may be compared with 1.44 Å for the usual C−O bond length in ethers (Supporting Information Tables S11 and S15). A methyl substituent at the anomeric carbon lengthens the C3(4)−O bonds with respect to the parent system by an average of 0.008 Å. Geminal methyl groups lead to further lengthening of those bonds. A different trend is observed when a bulky *tert*-butyl substituent is present at the anomeric carbon. One of the two C3(4)−O bonds has the same length as in **1a**/**2a**, while the other one is longer by ca. 0.016 Å. These changes suggest that both steric and stereoelectronic factors may determine the ground-state conformation.

B. Calculation of ^{13}C NMR Spectra. Shielding constants were calculated using the GIAO-DFT method at the mPW1PW91/6-311G(d,p) level of theory. This combination of basis set and density functional was chosen on the basis of our earlier, extensive studies on acetal compounds with well-established conformations. This investigation allowed us to find an empirical formula for calculation of ^{13}C chemical shifts:[24]

$$\delta = -0.96636 \cdot \sigma + 181.236 \text{ (ppm)}$$

where σ is the isotropic shielding constant obtained from quantum chemical calculations.

The δ values derived from experimental spectra were compared with calculated chemical shifts for sets of conformers with population exceeding 5% (for the Boltzmann distributions, see Table 1).

The molecules of investigated compounds under the conditions applied for NMR measurements are involved in fast conformational processes leading to time-averaged spectra. Thus, for calculated ^{13}C chemical shifts we have used an arithmetic average of δ of mutually exchanging carbon nuclei. This applies only to the compounds **1c**/**2c** (exchanging methyl groups), **1d**/**2d** (methyl groups in a rotating *tert*-butyl substituent), and **2a**−**d** (pairwise exchange of C1/C7, and C2/C6 nuclei). The calculated GIAO isotropic chemical shifts and experimental data for all carbon nuclei in **1a** are presented in Table 2. The respective values for remaining compounds are included in Supporting Information.

Agreement between the calculated and experimental chemical shifts was evaluated on the basis of the following parameters: the maximum ($\lvert\Delta\delta\rvert_{max}$) and average ($\lvert\Delta\delta\rvert_{avg}$) values of the modulus of the chemical shift difference $\lvert\delta_{expt} - \delta_{calcd}\rvert$, and the standard deviation error and correlation coefficient r^2 of the regression $\delta_{expt} = a + b\,\delta_{calcd}$. In our previous investigation of acetals, the value of $\lvert\Delta\delta\rvert_{avg}$ and the regression error were 0.97 and 1.27 ppm, respectively. The correlation coefficient was slightly greater than 0.998; the largest discrepancies between the calculated and experimental chemical shifts did not exceed 3.67 ppm.[24] Thus, if calculated spectra are described as matching the experimental ones, then comparison of these statistics should yield similarly close agreement.

The acetal **1a** exists as a mixture of three conformers, with the ground-state conformation populated to the extent of 83% (Table 1). Also, it was the global minimum of this compound that was found to have the calculated spectrum closest to the experimental one. The next two conformations have values of $\lvert\Delta\delta\rvert_{avg}$ and regression error 2−3 times worse, and almost 3−4 times greater maximum deviations (Table 2). In the third

conformer, chemical shifts of C1 and C5 are in reverse order. Values of the correlation coefficient are in line with the above findings. If the spectra of these three conformers are averaged over the Boltzmann distribution the agreement with the experimental data is improved. The improvement is quantified by the maximum deviation and regression error values, which are smaller by ca. 30−40%.

The monomethyl derivative **1b** is represented by two conformers of the same type, but with the opposite orientation of the substituent (Table 1). Neither of them, if treated separately, gives acceptable agreement between the experimental and calculated spectrum (Supporting Information Table S20). The maximum deviations are equal to almost 4 ppm, and other parameters with the exception of r^2 are also unsatisfactory. However, if the spectra of these conformations are averaged using their relative fractions, the resulting spectrum is very close to the one measured experimentally. The largest improvement is observed for the C1 and C5 carbons; depending on the conformation, one of them is upfield-shifted due to the γ-gauche effect from the methyl group, and the other is not. After averaging, these effects are balanced out, leading to much better agreement, as good as that achieved for **1a**.

Acetal **1c** is the only one of our 2,4-benzodioxonine derivatives that exists as a single conformer. Its calculated spectrum agrees very well with the experimental one over the whole range of chemical shifts (Supporting Information Table S21). The parameters of the match are close to those obtained for **1a** and **1b**.

The most conformationally complex derivative is acetal **1d**. On the basis of calculated energies, we found that five conformers have populations above 5%. Their individual calculated spectra are far from being close to the experimental one (Supporting Information Table S22). The maximum chemical shift difference does not fall below 5 ppm, and for C5 in the fifth conformer it reaches 12.6 ppm. Regression error and mean deviation in each case exceed 2.0 and 1.7 ppm, respectively. The averaged spectrum, however, displays a marked improvement over the individual conformers. Now, mean and regression errors are of the order of 1.0 ppm, r^2 is close to unity, and the maximum deviation is 2.8 ppm. The value of the last of the above parameters corresponds to the chemical shift difference associated with the quaternary carbon of the *tert*-butyl substituent, which is downfield-shifted in all cases.

For compounds **1a**−**d**, in general, the calculated spectra gave a satisfactory agreement with the experimental data, as confirmed by uniform values of statistical parameters describing their correlation. Theoretical chemical shifts were usually within 1.4 ppm from their experimentally measured counterparts, with the exception of carbons C6 and C7. Values calculated for these two nuclei were almost systematically predicted 1.8−2.3 ppm downfield from the expected δ.

The unsubstituted derivative of 3,5-benzodioxonine **2a** is represented by a single conformer. The spectrum calculated for its ground-state conformation correlates very well with the experimental data, as indicated by values of mean error and regression error (both below 1 ppm) and r^2, which is almost equal to 1.0 (Supporting Information Table S23). The maximum deviation of 2.0 ppm was found for the exchanging pair of C1/C7 carbons. Essentially the same results were obtained for the *gem*-dimethyl derivative **2c**, which has only slightly worse agreement between theoretical and experimental chemical shift values (Supporting Information Table S25).

The two most populated conformers of the monomethyl derivative **2b** are representatives of the same conformation, but with an orientation opposite of that of the substituent. Both gave theoretical spectra that are essentially identical. Consequently, their match with the experimental data is almost the same (Supporting Information Table S24). The agreement is in both cases satisfactory, with statistical parameters almost as good as those for **2a**. However, as expected, Boltzmann averaging of these two calculated spectra has not given any significant improvement. In this instance, when all of the calculated and experimental spectra agree with each other, conclusions about the relative fractions of the two conformers can only be drawn from modeling energies.

Among the three conformers of **2d**, the best agreement with the experimental spectrum was found for the spectral data calculated for the ground-state conformation, which constitutes more than 50% of the population (Supporting Information Table S26). The maximum deviation parameter determined for this conformer is equal 2.9 ppm, a value rather large in comparison with other cases discussed earlier. Remaining statistical estimates (mean error and regression error) are much better and have values of 1.0 and 1.4 ppm, respectively. The third conformer gave similar agreement; however, its average error was 0.5 ppm worse than that of the global minimum. Boltzmann averaging of the theoretical spectra of these three conformers yielded improvement of the maximum deviation, regression error, and correlation coefficient over the respective values obtained for the ground-state conformation. Only the mean error parameter was worsened by 30%.

The above results show excellent agreement between experimental chemical shifts and spectra calculated for acetals in which only one conformer dominates the population of molecules. This was also true for compounds for which comparison was done for chemical shifts obtained by averaging of theoretical spectra over populations derived from Boltzmann distribution based on free energies determined for isolated molecules in the gas phase. This leads to the important conclusion that ground-state geometries and conformers' free energies determined from geometry modeling in vacuo properly describe the conformational situation observed in the $CDCl_3$ solution.

C. NBO Analysis. Application of the natural bond orbitals (NBO) analysis to the investigation of the anomeric effect (AE) gives a unique insight into the fundamental phenomena underlying the AE's origin. In this approach, the electronic wave function of the molecule is treated as a linear combination of localized orbitals, either Lewis occupied, or non-Lewis unoccupied. Examination of delocalizations between these orbitals and evaluation of the energies associated with their interactions is a common technique.[10−14,20b,32−36] It can be accomplished either by inspecting the electronic energy partitioning obtained from second-order perturbation theory[13,34] or by performing selective deletions of off-diagonal elements of the Fock matrix.[12,33]

The oxygen lone pair donor orbital may participate in

(32) Cramer, C. J.; Kelterer, A.-M.; French, A. D. *J. Comput. Chem.* **2001**, *22*, 1194−1204.
(33) Moon, S.; Kwon, Y.; Lee, J.; Choo, J. *J. Phys. Chem. A* **2001**, *105*, 3221−3225.
(34) Roohi, H.; Ebrahimi, A. *J. Mol. Struct. (THEOCHEM)* **2005**, *726*, 141−148.
(35) Cuevas, G.; Juaristi, E.; Vela, A. *J. Phys. Chem. A* **1999**, *103*, 932−937.
(36) Tormena, C. F.; Rittner, R.; Contreras, R. H.; Peralta, J. E. *J. Phys. Chem. A* **2004**, *108*, 7762−7768.

TABLE 3. Relative HF−SCF Electronic Energies (ΔE_{tot}), Individual $n_O \rightarrow \sigma_{C-O}^*$ Contributions to Delocalization Energies from n_{sp} and n_p Donors, Total Delocalization Energies Resulting from $n_O \rightarrow \sigma_{C-O}^*$ Interactions (ΔE_{del}), and Their Relative Values Determined for Selected Conformers of Compounds 1a−d[a]

	conformer	ΔE_{tot}	$n_{sp,O2}$[b]	$n_{p,O2}$[b]	$n_{sp,O4}$[b]	$n_{p,O4}$[b]	ΔE_{del}[b]	$\Delta\Delta E_{del}$[b]	ΔE_{del}[c]	$\Delta\Delta E_{del}$[c]
1a	1, TBC(−)	0.00	−5.19	−67.11	−5.94	−66.19	−144.43	0.00	−108.30	0.00
	2, TCBtype-2(+)	7.19		−78.41	−4.85	−70.50	−153.76	-9.33	−114.92	−6.61
	3, SCBtype-3	7.63	−4.02	−72.13	−2.89	−76.07	−155.10	−10.67	−115.66	−7.35
...										
	14, TCBtype-1(−)	36.53		−83.68	−3.60	−76.48	−163.76	−19.33	−122.27	−13.97
1b	1, TBC(−)	0.00	−4.35	−70.84	−8.58	−60.54	−144.31	0.00	−106.33	0.00
	2, TBC(−)	1.21	−8.24	−58.12	-4.64	−72.01	−143.01	1.30	−105.34	0.99
	3, TCBtype-3(+)	10.30	−3.51	−53.43		−86.02	−142.97	1.34	−104.33	2.01
	4, SCBtype-3	9.97	−6.69	−65.40		−79.29	−151.38	−7.07	−112.26	−5.92
	5, TCBtype-2(+)	10.39		−78.49	−9.20	−57.49	−145.18	−0.88	−106.45	−0.11
...										
	17, TCBtype-1(−)	33.83		−83.22	−4.27	−74.56	−162.05	−17.74	−118.37	−12.03
1c	1, TBC(−)	0.00	−7.41	−62.76	−7.03	−67.53	−144.72	0.00	−104.79	0.00
...										
	7, SBBtype-1(+)	36.63	−2.22	−72.13	−2.34	−80.12	−156.82	−12.09	−111.93	−7.14
1d	1, TBC(−)	0.00	−3.01	−77.40	−12.89	−47.82	−141.13	0.00	−104.84	0.00
	2, TCBtype-3(+)	1.33	−4.10	−53.93		−85.35	−143.39	−2.26	−105.11	−0.27
	3, TBC(−)	0.95	−12.84	−43.43	−2.89	−78.49	−137.65	3.47	−102.11	2.73
	4, SCBtype-1	3.20	−9.71	−55.90	−5.31	−50.88	−121.80	19.33	−90.06	14.78
	5, TCCtype-1(−)	6.21	−3.93	−71.67	−3.47	−59.91	−138.99	2.13	−102.10	2.74
	6, TCBtype-1(+)	8.15	−3.47	−61.21	−11.88	−51.63	−128.20	12.93	−94.87	9.97
	7, TCBtype-2(+)	9.44		−76.90	−15.86	−38.79	−131.54	9.58	−97.65	7.19
	8, SCBtype-3	11.46	−11.13	−52.13		−81.88	−145.14	−4.02	−107.89	−3.05
...										
	25, TCTC(−)	88.74	−2.22	−81.38	−3.85	−74.39	−161.84	−20.71	−118.55	−13.71

[a] All values in kJ/mol. [b] Estimates from the second-order perturbation theory. Values below 2.1 kJ/mol are not shown. [c] Values calculated by deletion of specific off-diagonal elements of the Fock matrix.

TABLE 4. Relative HF−SCF Electronic Energies (ΔE_{tot}), Individual $n_O \rightarrow \sigma_{C-O}^*$ Contributions to Delocalization Energies from n_{sp} and n_p Donors, Total Delocalization Energies Resulting from $n_O \rightarrow \sigma_{C-O}^*$ Interactions (ΔE_{del}), and Their Relative Values Determined for Selected Conformers of Compounds 2a−d[a]

	conformer	ΔE_{tot}	$n_{sp,O3}$[b]	$n_{p,O3}$[b]	$n_{sp,O5}$[b]	$n_{p,O5}$[b]	ΔE_{del}[b]	$\Delta\Delta E_{del}$[b]	ΔE_{del}[c]	$\Delta\Delta E_{del}$[c]
2a	1, TCBtype-1	0.00	−3.22	−75.31	−2.93	−78.20	−159.66	0.00	−119.03	0.00
...										
	6, TCBtype-3	34.84		−83.01		−83.97	−166.98	−7.32	−124.88	−5.85
2b	1, TCBtype-1	0.00	−6.23	−67.20		−81.59	−155.02	0.00	−114.61	0.00
	2, TCBtype-1	2.45	−2.51	−77.78	−4.23	−74.31	−158.82	−3.81	−116.12	−1.51
...										
	17, SCBtype-3	52.86	−3.89	−80.17	−3.89	−80.17	−168.11	−13.10	−122.85	−8.24
2c	1, TCBtype-1	0.00	−5.61	−69.91	−2.30	−79.29	−157.11	0.00	−112.75	0.00
...										
	6, TCBtype-3	37.52	−4.77	−74.10		−85.23	−164.10	−6.99	−117.37	−4.62
2d	1, TCBtype-1	0.00	−10.79	−53.47		−82.63	−146.90	0.00	−108.91	0.00
	2, SCC	4.69		−67.49	−3.31	−76.02	−146.82	0.08	−108.47	0.44
	3, TCCtype-1	4.53	−8.37	−41.30		−83.26	−132.93	13.97	−97.44	11.47
	4, TCBtype-1	8.37		−80.83	−6.65	−67.78	−155.27	−8.37	−115.48	−6.56
	5, TCBtype-3	12.77		−82.09		−80.79	−162.88	−15.98	−119.93	−11.02
	6, TCBtype-2	10.37	−13.85	−42.22	−2.38	−64.22	−122.67	24.23	−90.75	18.16
...										
	14, SCBtype-3	41.37	-3.51	−79.91	−3.51	−79.91	−166.86	−19.96	−122.55	−13.64

[a] All values in kJ/mol. [b] Estimates from the second-order perturbation theory. Values below 2.1 kJ/mol are not shown. [c] Values calculated by deletion of specific off-diagonal elements of the Fock matrix.

interactions with C−O, C−H, and C−C antibonding orbitals. For the AE in acetals, four delocalizations to the vicinal σ_{C-O}^* antibonding orbital are responsible.[10,33] The approach using the NBO analysis in which the $n_O \rightarrow \sigma_{C-O}^*$ interactions and their energies are treated separately from others has the following advantages: (1) it focuses on the simplest delocalizations that are unique for acetals, (2) values of the stabilization energies and their variations over a series of conformers are not overshadowed by others related to stronger delocalizations such as those in an aromatic ring, and (3) comparison of stabilization energies calculated in this way can be done between molecules of different acetals and with various other functional groups.[33]

The results of the NBO analysis performed for compounds **1a−d** and **2a−d** are summarized in Tables 3 and 4. All conformers presented there are characterized by their total electronic energies obtained from the HF−SCF single-point calculations (ΔE_{tot}), along with stabilization energies (ΔE_{del}) and their relative values ($\Delta\Delta E_{del}$) derived either from the second-order perturbation theory or from deletion of the $n_O \rightarrow \sigma_{C-O}^*$ interactions. In all cases, the second-order perturbation theory estimates of ΔE_{del} exceed values obtained from selective deletions by some 33−35%, but otherwise they follow the same trend. Delocalization energies of individual interactions are also shown, unless they do not exceed ca. 2 kJ/mol. One of the lone pairs occupies an sp^n hybrid orbital with the *p*-character in a

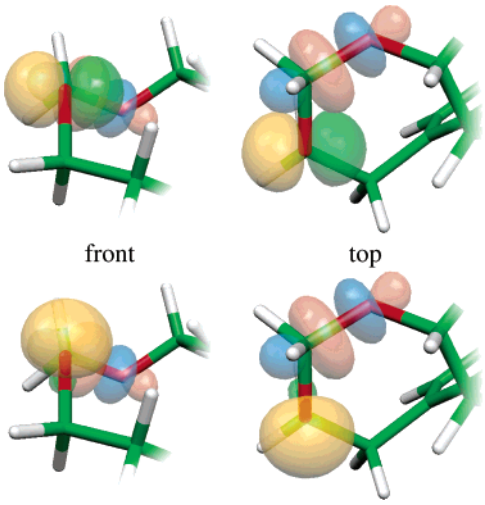

FIGURE 1. Front- and top-side projections of the interaction between the σ_{C-O}* orbital (blue/orange) and the *p*-type (top row) or the sp^n-type lone pair (bottom row) in the global minimum of **2a**. NBO−HF/6-31G** (O, 6-31+G*)//B3LYP/6-31G** (O, 6-31+G*).

range of 60−64% (n_{sp}), while the other has an almost pure *p*-type orbital (n_p). This is true for both oxygen atoms.

The energy values of lone pair interactions listed in Tables 3 and 4 are greater for n_p than for n_{sp} orbitals (e.g., compare −5.19 and −67.11 kJ/mol for the O-2 in the global minimum of **1a**). In other words, the orbital interactions in which the n_p lone pairs participate stabilize the energy more extensively than those in which the sp^n-type hybrids take part. The explanation for this can be derived from the following: (1) the n_p orbitals have higher energy than n_{sp} (−0.47 au vs −0.77 au) and consequently there is a smaller energy gap between the donor and acceptor, and (2) the mutual spatial arrangements of the n_p pair and the antibonding orbitals allow their more efficient interaction (Figure 1).

Let us turn our attention to the *p*-type lone pair interactions in the ground-state conformations of acetals **1** and **2**. In both the TBC and TCBtype-1 conformations, the acetal moiety has the $g\pm g\pm$ orientation. For the unsubstituted systems, respective energy values for both n_p pairs do not differ by more than a few kJ/mol, and in the dimethyl derivatives these energy differences do not exceed 10 kJ/mol. This is reflected in bond lengths in the O−C−O fragment, which agree within 0.004 Å (Supporting Information Tables S11−S18). However, when there is a single substituent at the anomeric carbon, the energy differences are greater than 10 and 29 kJ/mol for the monomethyl and *tert*-butyl derivatives, respectively. As expected, the related bond length deviations are also greater and equal to 0.006−0.010 Å for **1b**/**2b** and 0.014−0.017 Å for **1d**/**2d**, with the shorter bond on the side with stronger stabilization. Examination of the ground-state geometries of the monosubstituted acetals made it possible to rationalize the observed asymmetry: the longer of the two C−O bonds is the one that connects the anomeric carbon with the O−CH_2 fragment being gauche to the alkyl substituent. When the geometrical features of global minima of compounds with the methyl and *tert*-butyl groups at the anomeric carbon are compared (**1b**/**1d** and **2b**/**2d**), the increased steric hindrance from the *tert*-butyl substituent causes the exocyclic torsion angle R−C−O−CH_2 to become greater and the endocyclic O−CR−O−CH_2 angle to become somewhat smaller. These structural changes, together with above-mentioned bond lengthening, cause worse overlap of donor and acceptor orbitals and smaller stabilization energies. Thus, steric congestion leads to substantial changes in the hyperconjugative stabilization of the conformations. This is an extension of the statement made in the last paragraph of section A.

If we consider the total stabilization energies ΔE_{del} determined for the ground-state conformations of compounds **1** and **2**, two things can be noted. First, for any of the global minima of **2** the ΔE_{del} is greater than that in **1**, even though in either case the acetal moiety has the $g\pm g\pm$ atom arrangement. The possible explanation for this asymmetry may be built upon subtle differences in the values of the C−O−C−O−C torsion angles between both groups of acetals; in the global minima of **1** their average values are approximately −56°, while in **2** they are greater and lie in a range of −64 to −68°. As will be shown in the following section, this directly translates into stronger hyperconjugative stabilization.

Second, in both families of acetals the values of ΔE_{del} in ground-state conformations diminish with the number and size of the substituents at the anomeric carbon. The highest stabilization energy is observed for the nonsubstituted system. With introduction of one or two methyl substituents, ΔE_{del} is systematically decreased and reaches minimum value for the derivative substituted with the bulky *tert*-butyl group. This trend stems from the previously discussed effect related to steric crowding introduced by the alkyl substituents, which affects the effectiveness of the donor and acceptor orbital overlap. The effect of the substitution is also greater for **2** than for **1**. The ΔE_{del} difference between the unsubstituted and the *tert*-butyl derivatives is 10 kJ/mol in the former and 3.5 kJ/mol in the latter.

To obtain better insight into the stereoelectronic effect in acetals, let us now compare the ΔE_{del} stabilization energies between the ground-state and higher-energy conformations. First we will narrow the scope of this discussion to the conformers with free energies in a 10 kJ/mol window, a condition that selects conformations having non-negligible population fractions. If we examine the three derivatives **1a**, **1b**, and **1d**, which permit such analysis, then in each case there are conformations within the imposed free-energy limit that exhibit stronger anomeric stabilization. These are the two next higher energy conformers of **1a**, the fourth and fifth conformer of **1b**, and the second and eighth conformer of **1d**. Closer examination reveals that the highest value of ΔE_{del} is in either case displayed by the SCBtype-3 conformation. An analogous analysis can be done only for **2b** and **2d** derivatives of 3,5-benzodioxonine. For the former, the only conformer available for comparison is also the one with stronger anomeric stabilization. It is the conformation of the same type as the global minimum, but with the opposite orientation of the methyl group. For **2d** there are two conformers with higher ΔE_{del}: the first, similar as in **2b**, represents the same conformation as the global minimum, but differs in the orientation of the substituent (no. 3), the other, fifth in free energy, is an example of the TCBtype-3 conformation.

The above findings indicate that in each of the present acetals, if there are conformers within the 10 kJ/mol free-energy window to compare with the ground-state conformation, then at least for one of them stronger anomeric stabilization than that in the global minimum is observed.

If we extend the scope of this discussion to all conformers of the title compounds, then analysis similar to that performed above leads to a more general observation, that in neither case

the global minimum displays the strongest stabilization due to the $n_O \rightarrow \sigma_{C-O}^*$ interactions. Among the derivatives of 2,4-benzodioxonine, the highest values of ΔE_{del} are found in conformers TCBtype-1 (**1a**,14 and **1b**,17), SBBtype-1 (**1c**,7), and TCTC (**1d**,25). In the case of the first two compounds, the TCBtype-1 conformation has ΔE_{del} greater than the nearest following minima by ca. 4 kJ/mol, in marked contrast with compounds **1c** and **1d**, where there are at least three highly stabilized conformations within a range of 2 kJ/mol of the peak ΔE_{del} value.

In the family of compounds **2a**−**d**, the highest values of stabilization energy due to the anomeric $n_O \rightarrow \sigma_{C-O}^*$ interactions are present for the two nine-membered ring conformations, namely TCBtype-3 and SCBtype-3. For the former, the strongest donor−acceptor delocalizations exist in compounds **2a** and **2c**. Additionally, in **2a** TCBtype-3 (no. 6) is directly followed by the SCBtype-3 conformation (no. 12), whose stabilization energy is lower by only 0.09 kJ/mol. In the other two compounds (monosubstituted systems **2b** and **2d**) the order is reversed and the SCBtype-3 conformation (**2b**,17 and **2d**,14) has the strongest AE interactions. The TCBtype-3 conformation displays the second highest stabilization energy values, 1.82 and 2.62 kJ/mol lower, respectively (**2b**,7 and **2d**,5).

Regardless of the type of conformation discussed above, each of the conformers with the highest value of ΔE_{del} has free energies well above those of the ground-state conformation. This is due to the dominating steric repulsive interactions, which despite the favorable stereoelectronic interactions raise the energy of the conformation to a level that prohibits detection by means of any experimental method.

Having established the energetic effects of the stereoelectronic interactions present in molecules of the investigated compounds, let us now consider how the ΔE_{del} energies translate into values of C−O−C−O−C torsion angles. On this basis the conformations with the strongest anomeric stabilization can be divided into two categories. The first and largest group includes conformers in which the discussed torsion angles have opposite signs and one or both of them are close to 90°. Among its members are conformations TCBtype-1 of **1a**,**b**, TCTC of **1d**, and TCBtype-3 of **2a**,**c**. It was noted before by Cramer et al.[32] that the strongest interaction of the *p*-type lone pair with the acceptor C−O antibonding orbital occurs for the orthogonal torsion angle, when the donor and acceptor are periplanar. Since the n_p pair interaction energy is the dominating term of ΔE_{del}, then this explains the observed structural pattern. The other group consists of conformers possessing the $g\pm g\pm$ or $g+g-$ arrangement of the atoms in the acetal moiety (SBBtype-1 of **1c**, SCBtype-3 of **2b**,**d**). Here neither of the two angles is orthogonal, but ΔE_{del} is additionally supported by the non-negligible n_{sp}-originating terms.

The above discussion allows us to state that, although in all of the ground-state conformations the acetal moiety adopted the $g\pm g\pm$ geometry that is typical for the generalized anomeric effect, the respective ΔE_{del} value was found to be greater for conformers higher in energy. The fact that the majority of acetal fragments in these conformers possessed other types of geometry, such as $g+g-$ (e.g., SCBtype-3 in **2**) or the *anomeric eclipsed* (e.g., TCBtype-1(−) in **1**), leads to our conclusion that strong AE stabilization is not restricted to the $g\pm g\pm$ arrangement only.

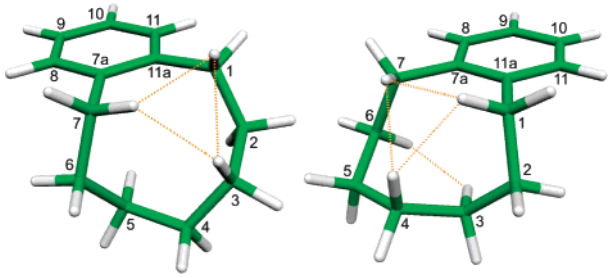

FIGURE 2. Numbering of atoms in the TCBtype-1 and TBC conformations of benzocyclononene and distances between hydrogens involved in transannular interactions (values in Å from DFT geometry modeling).

D. Stabilization of the Ground-State Conformations. Molecules of compounds **2** adopted the same ground-state conformation as the molecules of the parent hydrocarbon, whereas for compounds **1** the second in energy conformer of the carbocycle is preferred. In the molecule of benzocyclononene, the main factor influencing the relative stabilities of its conformers is the steric effect. Among them the transannular interactions usually play an important role and may be easily analyzed by inspection of calculated geometries. In the TCBtype-1 conformation, there are three H···H interactions between hydrogens at the C1, C3, and C7 carbon atoms (Figure 2). Four such interactions exist in the TBC conformation: three on one side of the ring between hydrogens at C1, C4, and C7, and one on the other side between hydrogens in the C3 and C6 positions. In compounds **2** there is a release of two transannular interactions in the TCBtype-1 conformation upon introduction of two oxygen atoms in place of C3 and C5. After introduction of two oxygen atoms in TCBtype-1 in positions C2 or C6, and C4, none of the transannular interactions is removed, whereas in the TBC conformer three such interactions are avoided. That analysis clearly shows that repulsive steric interactions are the main factor determining the conformation of the global minima. On the other hand, discussed structural features, namely torsion angles and bond lengths within the acetal moiety, and most importantly the stabilization due to the $n_O \rightarrow \sigma_{C-O}^*$ delocalizations, enable us to state that the stereoelectronic effect is also an important factor participating in the stabilization of the ground-state conformations.

Conclusions

In the process of the conformational analysis we have determined the geometries of the ground-state conformations of these acetals. In either case the acetal moiety adopts the $g\pm g\pm$ arrangement. Analysis of hyperconjugative orbital interactions derived from NBO calculations has shown that the strongest stabilization due to the stereoelectronic $n_O \rightarrow \sigma_{C-O}^*$ delocalizations is achieved when the C−O−C−O torsion angles are

close to 90°, similar to findings for 2,4,6-trioxaheptane by Cramer et al.[32] It is a consequence of a domination of the *p*-type lone-pair interaction with the σ_{C-O}* antibonding orbital, which is the strongest when both the donor and acceptor are periplanar. The above condition, however, was not fulfilled in either of the ground-state conformations. The global minima of compounds **1** and **2** are the TBC and TCBtype-1 conformations, respectively, the latter being also the most stable conformation of the parent carbocycle. Examination of the geometries of the ground-state conformations showed that, among others, avoiding the transannular interactions is responsible for the conformational preferences. Investigation of the structural features and stereoelectronic interactions present in the ground-state conformations allowed us to state that the conformational preferences of these acetals stem from the balance of both steric and hyperconjugative effects, namely $n_O \rightarrow \sigma_{C-O}$* delocalizations.

The methodology used in the process of the conformational analysis, which was set up upon the DFT geometry modeling and simulation of NMR spectra of isolated molecules, proved to be an adequate tool that provided correct information about conformational preferences and equilibria of molecules of cyclic acetals in $CDCl_3$ solution.

Experimental Methods

NMR Measurements. ^1H and ^{13}C NMR spectra were recorded at 500.13 and 125.76 MHz, respectively, for 0.15 mg/mL solutions in $CDCl_3$ at 300 K. Chemical shifts were referenced to either TMS (^1H) or $CDCl_3$ (^{13}C). The COSY, HETCOR, and HMBC spectra were recorded at 11.7 or 7.0 T using standard Bruker procedures.

Acknowledgment. We thank the ACK Cyfronet for generous allocation of computing time on the SGI 2800 workstation (Grant No. KBN/SGI2800/UJ/002/2003).

Supporting Information Available: Detailed synthetic procedures. NMR spectra. Free energies, enthalpies, total electronic energies, lowest mode frequencies, torsion angles, C−O−C bond lengths (acetals only), and atomic coordinates from DFT calculations for all conformers of benzocyclononene and compounds **1** and **2**. Comparison of experimental and calculated ^{13}C chemical shifts. Total electronic HF−SCF energies, energies of n_{sp} and n_p lone pair delocalizations, and ΔE_{del} for all conformers of compounds **1** and **2**. This material is available free of charge via the Internet at http://pubs.acs.org.

JO060422C